Journal of the European Ceramic Society **14** (1994) 411–418

Nitridation of SiC for the Production of $SiC–Si_3N_4$ Nanocomposites

E. Gomez, T. Gómez-Acebo, J. Echeberría, I. Iturriza & F. Castro

Centro de Estudios e Investigaciones, Técnicas de Guipúzcoa (CEIT),
P° Manuel de Lardizábal 15, 20009 San Sebastián, Spain

(Received 5 December 1993; revised version received 10 May 1994; accepted 24 May 1994)

Abstract

High pressure sintering of SiC green compacts, both with and without additions of Al_2O_3 *and* SiO_2*, has been carried out in a HIP press under a nitrogen atmosphere. The amount of conversion of SiC to* Si_3N_4 *has been quantified after nitridation by XRD, and the results were interpreted in terms of phase stability diagrams taking into account the chemical composition of the specimens, the carbon activity and the nitrogen and the oxygen partial pressure. As a result of the process the final microstructure of the sintered materials was observed to consist of a combination of SiC and* Si_3N_4 *grains in the nanosize range and whose relative volume fractions depend on sintering conditions and the initial chemical composition. A minor proportion of free carbon, in the form of both amorphous carbon and nanosized graphite grains, was also part of the microstructure. This method is therefore regarded as a means for the production of* $SiC–Si_3N_4$ *nanocomposites with varying amounts of SiC,* α*-*Si_3N_4 *and* β*-*Si_3N_4

SiC-Grünlinge mit und ohne SiO_2 *und* Al_2O_3*-Zusatz wurden bei hohem Druck in einer HIP-Presse unter Stickstoffatmosphäre gesintert. Die Menge an SiC, das sich in* Si_3N_4 *unwandelt, wurde nach der Nitrierung mit Hilfe von XRD bestimmt und die Ergebnisse bezüglich der Phasenstabilitätsdiagramme unter Berücksichtigung der chemischen Zusammensetzung der Proben, der Kohlenstoffaktivität und der Stickstoff- und Sauerstoffpartialdrücke interpretiert. Das Gefüge der gesinterten Proben bestand als Resultat der Prozeßbedingungen aus einer Kombination von SiC- und* Si_3N_4*-Körnern, deren Größe einige Nanometer beträgt, und deren Volumenanteil von den Sinterbedingungen und der chemischen Zusammensetzung des Ausgangsmaterials abhängt. Ein geringer Teil des freien Kohlenstoffs, in Form von amorphem Kohlenstoff und nanometergroßen Graphitkörnern, ist Bestandteil des Gefüges. Diese Herstellungsmethode kann deshalb zur Produktion von SiC-*Si_3N_4*-Nanoverbindungen mit unterschiedlichen Anteilen von SiC,* α*-*Si_3N_4 *und* β*-*Si_3N_4 *eingesetzt werden.*

On a fritté des pastilles brutes de SiC, contenant ou ne contenant pas d'Al_2O_3 *et* SiO_2 *comme additifs, ceci par pressage isostatique à chaud (HIP), sous azote. Après nitruration, le taux de conversion de SiC en* Si_3N_4 *a été déterminé par diffraction X, et les résultats interprétés en termes de diagrammes de phases, en tenant compte de la composition chimique des échantillons, de l'activité du carbone, des pressions partielles d'azote et d'oxygène. La microsctructure finale des produits frittés est un mélange de grains de SiC et* Si_3N_4*, de taille nanométrique, et dont les fractions volumiques relatives dépendent des conditions de frittage et de la composition initiale. On trouve également du carbone libre, soit amorphe soit sous forme de grains de graphite nanometriques, en petite quantite. Cette méthode semble donc adéquate pour produire des nanocomposites* $SiCSi_3N_4$ *contenant des quantités variables de SiC,* α*-*Si_3N_4 *et* β*-*Si_3N_4*.*

1 Introduction

Silicon carbide and silicon nitride based ceramics have been extensively studied[1–5] particularly because of their excellent mechanical properties at high temperatures. While Si_3N_4 and SiC monolithic ceramics exhibit very attractive properties themselves, the design of Si_3N_4–SiC composite materials has attracted attention mainly due to their improved high temperature strength and increased fracture toughness.[6–9] The fabrication of Si_3N_4–SiC composites has been tried using SiC whiskers, fibres, platelets and a dispersion of particles for the rein-

Journal of the European Ceramic Society 0955-2219/94/$7.00

forcement of Si_3N_4.[6–11] In most of these cases densification has been achieved by the application of high pressure through hot pressing or HIPing, since pressureless sintering rates have been observed to decrease considerably due to the presence of the hard non-sinterable crystals of the second phase.[11,12] Si_3N_4–SiC composite materials have also been obtained by a reaction bonding route or mechanical attrition through the use of dispersants.[7,12–14]

Additional interest in composite materials is based upon the fabrication of very small grain sized ceramics, particularly in the nanosize range. Work in this area has been focused on the use of mechanical attrition[15] and hot pressing of CVD Si–C–N amorphous powders[16,17] together with metal oxide additions to aid densification.

The present paper reports on the obtention of Si_3N_4–SiC nanocomposites by the nitridation of SiC-based green compacts through hot isostatic pressing. The method looks promising not only because of the formation of nanosize microstructures but also because densification takes place with little or without any shrinkage at all. Some thermodynamic aspects related to the nitridation of SiC in a high pressure nitrogen atmosphere are discussed.

2 Experiment Procedure

The basic powders used during this work were Superior Graphite HCS059 and Lonza UFB10 SiC grades, precipitated silica (BDH Ltd, Poole, UK) and Alcoa CT 3000 SG Al_2O_3. Powder mixtures consisting of SiC + (10 or 30) wt% SiO_2 and SiC + 5 wt% Al_2O_3 were obtained after dry milling/mixing in a ball mill with SiC milling media. Cylindrical green compacts prepared from these powder blends, and also from SiC powders in the as-received condition of 5 mm height and diameters in the range of 10 to 20 mm, were produced by cold isostatic pressing at 100 MPa. Sintering was carried out in nitrogen (99·995% pure) between 1400 and 1850°C within a pressure range from 0·5 to 200 MPa, and holding times up to 90 min in a ASEA Q1H-6 HIP equipment. After sintering the specimens were weighed and measured in order to determine weight changes and amount of shrinkage. Their density was obtained by the immersion method. The quantitative determination of the phases present in the as-sintered samples was carried out by standard XRD methods[18] using Cu-α radiation. XRD work was carried out, both on the surface of the specimens and after cutting to expose a plane parallel to the base of the cylinders and passing through their centre. Discs 3 mm in diameter were cut out from a selection of specimens and subsequently ion-beam thinned to be examined under the transmission electron microscope.

3 Results

The stability of SiC during sintering of silicon carbide green compacts in a nitrogen atmosphere was observed to show a strong dependence on both temperature and pressure. Under these conditions conversion of SiC into Si_3N_4 may occur according to the following chemical reaction:

$$3SiC + 2N_2 \Leftrightarrow Si_3N_4 + 3C \qquad (1)$$

In the present work it was observed that the equilibrium shifts to the right in reaction (1) at temperatures above 1450°C and pressures higher than 5 MPa.

As a means of illustration Fig. 1 shows the phases observed in two specimens after sintering at (a) 1400°C and 50 MPa, and (b) 1750°C and 50 MPa. The XRD traces clearly show that the nitridation of silicon carbide leads to the formation of silicon nitride in both forms, that is, α- and β-Si_3N_4 (Fig. 1(b)).

Although the nitridation process was observed to take place all through the bulk of the powder compacts, the amount of conversion of SiC into Si_3N_4 was much larger on the surface, particularly

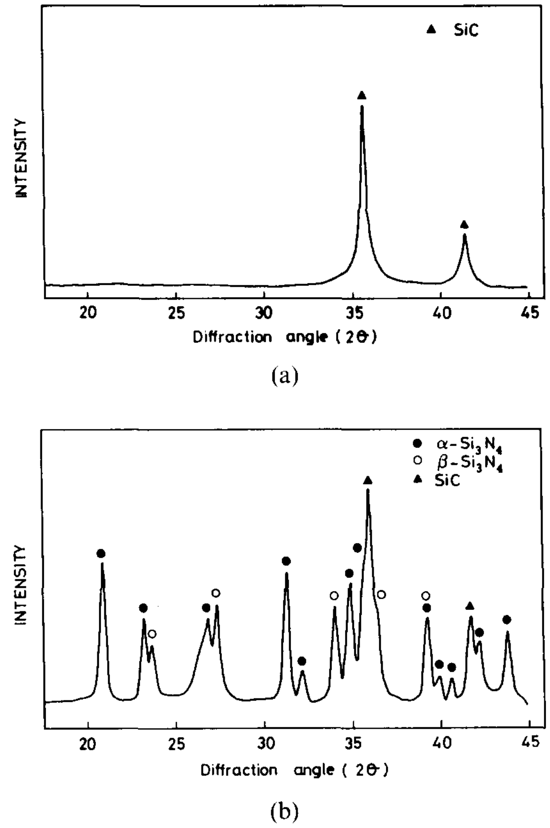

(a)

(b)

Fig. 1. XRD trace of a SiC compact sintered during 30 min under a pressure of 50 MPa N_2 at (a) 1400°C and (b) 1750°C.

Table 1. Quantitative results obtained from XRD traces after sintering of SiC powder compacts during 30 min under several combinations of temperature and pressure

Temperature (°C)	*Pressure (MPa)*				
	0·5	*5*	*50*	*75*	*200*
1 400	NC	NC	NC		
1 450	NC	NC	NC		
1 500	NC		S-65-35 I-81-19		
1 750	NC	S-27-73 I-85-15	S-17-83 I-13-87		S-20-80 I-11-89
1 800			S-20-80 I-0-100	S-20-80 I-0-100	
1 850		NC			

NC = no change observed, S = surface and I = interior. Numbers correspond to amounts measured for SiC (first number) and Si_3N_4 (second number).

when the sintering conditions were too close to the limiting temperature (1450°C) and pressure (5 MPa). Nevertheless, as seen in Table 1, which presents a summary of results obtained under various sintering conditions, the specimens exhibited a higher degree of homogeneity (comparing their surface and interior) as pressure and temperature were increased.

It is noteworthy that Table 1 only reports on the amounts of SiC and Si_3N_4 observed in the specimens, irrespective of the type of silicon nitride detected by XRD. The numbers in Table 1 corresponding to Si_3N_4 therefore represent the sum of $\alpha + \beta$ silicon nitride. In graphic form Fig. 2 shows the conversion of SiC into Si_3N_4 in percentage as a function of temperature and pressure. It is important to mention, however, that the amount of α-Si_3N_4 observed in all the specimens was surprisingly high. In fact, as observed in Fig. 3, the amount of α-Si_3N_4 in the specimens shows an increasing tendency with both temperature and pressure.

Irrespective of the type of Si_3N_4 formed, during conversion of SiC into Si_3N_4 according to reaction (1), it is clear that as nitrogen reacts with SiC a net weight gain will be produced (see Table 2).

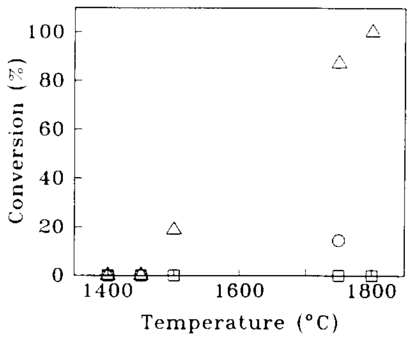

Fig. 2. Percentage of conversion of pure SiC to Si_3N_4 after sintering during 30 min under a N_2 pressure of □, 0·5 MPa; ○, 5 MPa; and Δ, 50 MPa.

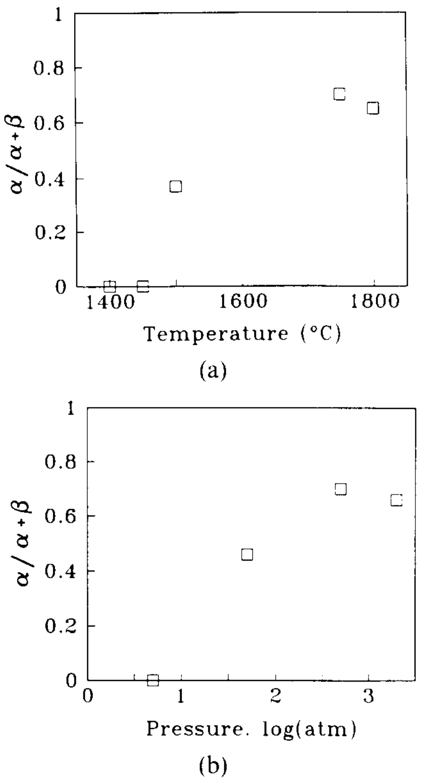

(a)

(b)

Fig. 3. $\alpha/\alpha + \beta$ ratio silicon nitride in pure SiC specimen sintered in a N_2 atmosphere (a) at a constant pressure of 50 MPa and (b) at a constant temperature of 1750°C.

Additionally, since the amount of shrinkage observed was negligible in all cases, this represents a non-shrinkage densification process for the preparation of SiC–Si_3N_4 composites. At 1750°C and 50 MPa pressure, for instance, a weight increase of ~38% was measured, thus obtaining a composite with a density of ~2·5 g/cm^3 and a Si_3N_4/SiC ratio of ~4 to 1.

In order to investigate the influence of SiO_2 and Al_2O_3 on densification, formation of Si_3N_4 and $\alpha \rightarrow \beta$ transformation, controlled amounts of these compounds were added to the raw SiC powders to obtain powder mixtures of SiC + 10 wt% SiO_2, SiC + 30 wt% SiO_2 and SiC 5 wt% Al_2O_3. As observed in Fig. 4 the additions of SiO_2 led to the formation of Si_2N_2O. The amounts of Si_2N_2O measured in the specimens for a fixed sintering time t were observed to depend on silica content, temperature and nitrogen pressure. These results

Table 2. Densities and weight gains of SiC compacts with additions of silica and alumina after sintering during 30 min at 1750°C and under several N_2 pressures

Additions to SiC	*Pressure (MPa)*			
	0·5	*5*	*50*	*200*
	ρ(g/cm^3); Δ wt(%)	ρ(g/cm^3); Δ wt(%)	ρ(g/cm^3); Δ wt(%)	ρ(g/cm^3); Δ wt(%)
0 wt% SiO_2	1·83; −0·8	2·013; 8·04	2·50; 38	2·54; 38
10 wt% SiO_2	1·75; −8·11	1·994; 7·74	2·453; 34·95	2·454; 36·62
5 wt% Al_2O_3	1·94; 6·54	2·251; 5·52	2·53; 28·02	2·83; 24·6

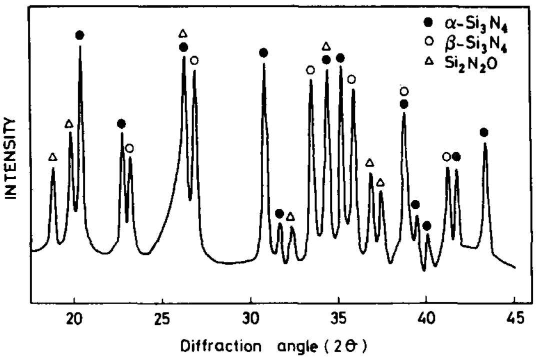

Fig. 4. XRD trace of a SiC + 10 wt% SiO_2 sample sintered during 30 min under a N_2 atmosphere at 1750°C and 50 MPa.

are illustrated in graphic form in Figs 5 and 6. In terms of temperature the amount of SiC remaining in the specimens, after nitridation at a pressure of 50 MPa, decreases markedly between 1450 and 1500°C to disappear completely at about 1750°C. The products into which SiC are converted vary in quantitative terms according to Figs 5(b) and 5(c). In the figures it is apparent that Si_2N_2O may be formed, in preference to Si_3N_4, either at low temperatures and low SiO_2 contents or at high temperatures and high SiO_2 contents.

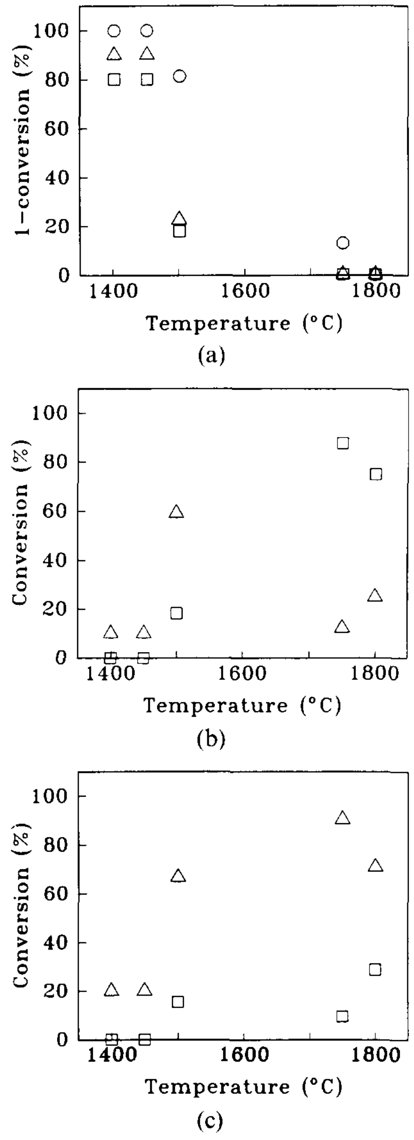

(a)

(b)

(c)

Fig. 5. (a) Residual SiC in samples containing: ○, SiC; Δ, SiC + 10 wt% SiO_2; and □, SiC + 30 wt% SiO_2, after sintering at 50 MPa N_2. Amounts of: □, Si_3N_4 and Δ, Si_2N_2O in (b) a SiC + 10 wt% SiO_2 specimen and (c) a SiC + 30 wt% SiO_2 specimen after sintering at 50 MPa in N_2 for 30 min.

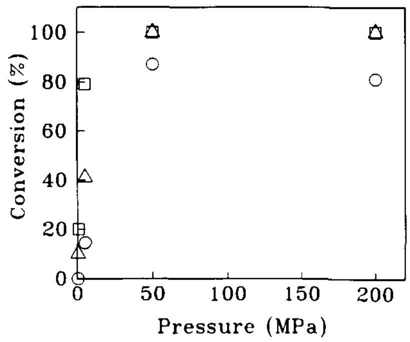

Fig. 6. Total amount of SiC converted into Si_3N_4 + Si_2N_2O in specimens of: ○, pure SiC, Δ, SiC + 10 wt.% SiO_2 and □, SiC + 30wt.% SiO_2.

The direct nitridation of silica may take place through the reaction

$$2\,SiO_2 + N_2 \Leftrightarrow Si_2N_2O + 3/2\,O_2 \qquad (2)$$

which seems to be favoured at low temperatures and low silica contents since, as temperature is increased, Si_3N_4 will be formed instead, due to a lower availability of oxygen (lower contents of SiO_2). At high temperatures, on the other hand, the formation of Si_2N_2O may take place by a sequence of Si_3N_4 formation and the following reaction

$$Si_3N_4 + SiO_2 \Leftrightarrow 2\,Si_2N_2O \qquad (3)$$

with the relative amounts of Si_3N_4 and Si_2N_2O formed being dependent on the amount of silica added to the powder mixture. It is worth mentioning that in this sequence the role of carbon is important, particularly at high silica contents, through the reduction of SiO_2 and the formation of volatile species (e.g. CO) which counterbalance the weight gains during nitridation, consequently leading to less dense specimens and mainly formed by Si_2N_2O. At 1750°C, Fig. 6 shows that the final amount of SiC in the specimens exhibits a strong dependence on N_2 pressure and SiO_2 content.

In contrast to the low density observed in specimens containing SiO_2, the addition of Al_2O_3 as sintering aid leads to nearly fully dense materials, as it is also typically observed during sintering of sialons and Si_3N_4.[19] The additions of Al_2O_3 were also observed to encourage the $\alpha \rightarrow \beta$ transformation leading to fully β-Si_3N_4–SiC composites.

On examination under the TEM the microstructure of these materials was observed to consist of grains and a minor fraction of amorphous areas (Fig. 7). Detailed observation of these specimens revealed that the amorphous areas corresponding to carbon and the grains, which represent at least

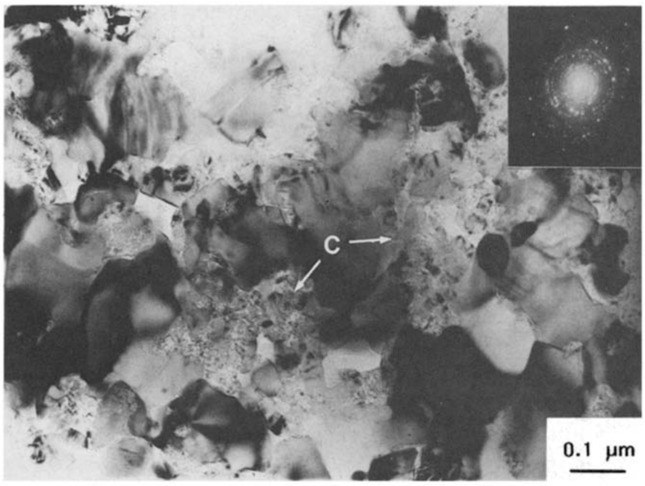

Fig. 7. TEM micrograph of a composite obtained after sintering a SiC green compact at 1750°C, 50 MPa N$_2$ without any holding time and electron diffraction pattern of crystalline carbon.

75 vol.% of the specimens, were silicon carbide and silicon nitride. The morphology of the grains was generally equiaxed and particularly in the case of Si$_3$N$_4$ grains, their size was below 50 nm, whereas the SiC grains were of about 100 nm. The distribution of SiC and Si$_3$N$_4$ grains in the microstructure was observed to be fairly uniform, thus indicating that the formation of Si$_3$N$_4$ grains took place by nucleation around SiC particles. The areas corresponding to carbon were also found relatively homogeneously distributed separating grains but not particularly as an intergranular phase. Detailed examination of these areas also revealed the presence in large amounts of extremely small (<10 nm) grains which were identified as crystalline carbon, according to the spotty appearance of the rings in the electron diffraction pattern (Fig. 7).

4 Discussion

According to these results and under the experimental conditions used in this work it can be observed that the phases in equilibrium after sintering of silicon carbide in a nitrogen atmosphere are α- and β-Si$_3$N$_4$, SiC and carbon. The chemical reactions that represent the equilibrium between these phases, in the present temperature range, may then be expressed as

$$3\text{SiC} + 2\text{N}_2 \Leftrightarrow \beta\text{-Si}_3\text{N}_4 + 3\text{C} \qquad (4)$$

and

$$3\text{SiC} + 2\text{N}_2 \Leftrightarrow \alpha\text{-Si}_3\text{N}_4 + 3\text{C} \qquad (5)$$

Following the approach reported by Wada *et al.*[20] and using the data compiled by Hendry (who considered α-Si$_3$N$_4$ as Si$_{11\cdot4}$N$_{15}$O$_{0\cdot3}$)[21] for the free energies of formation of these compounds in kJ/mol, that is, $\Delta G^0(\alpha\text{-Si}_3\text{N}_4) = -1167{\cdot}3 + 0{\cdot}594T$, $\Delta G^0(\beta\text{-Si}_3\text{N}_4) = -936 + 0{\cdot}45T$ and $\Delta G^0(\text{SiC}) = -72{\cdot}832 + 0{\cdot}007T$, eqn (5) should be rewritten as

$$\begin{aligned} &2{\cdot}85\text{SiC} + 1{\cdot}875\text{N}_2 + 0{\cdot}0375\text{O}_2 \\ &\Leftrightarrow 1/4\text{Si}_{11\cdot4}\text{N}_{15}\text{O}_{0\cdot3} + 2{\cdot}85\text{C} \qquad (5a) \end{aligned}$$

and the ratio of activities between Si$_3$N$_4$ and SiC may be calculated, as a function of P_{N2} and a_C, through the following relationships

$$\begin{aligned} &\log\left(\frac{a_{\beta\text{-Si}_3\text{N}_4}}{a_{\text{SiC}}{}^3}\right) \\ &= \frac{37\,480}{T} - 22{\cdot}41 - 3\log a_\text{C} + 2\log P_{\text{N}_2} \qquad (6) \end{aligned}$$

and

$$\begin{aligned} &\log\left(\frac{a_{\alpha\text{-Si}_3\text{N}_4}}{a_{\text{SiC}}{}^{2\cdot85}}\right) \\ &= \frac{50\,133}{T} - 29{\cdot}99 - 2{\cdot}85\log a_\text{C} \qquad (7) \\ &\quad + 1{\cdot}875\log P_{\text{N}_2} + 0{\cdot}0375\log P_{\text{O}_2} \end{aligned}$$

The results of these calculations for two of the sintering conditions used in this work (P_{N_2} = 0·5 and 50 MPa) are represented in graphic form in Fig. 8, considering $a_\text{C} = 1$, since the specimens were sintered on a graphite base and in a HIP press with a graphite heating element.

In terms of Fig. 8, it is interesting to observe, first of all, at a pressure of 0·5 MPa, that above 1783 K (1510°C) SiC is the stable phase. Therefore, it is clear, in accord with the numerical data shown in Table 1, that although the thermal activation could be thought to be high enough to convert SiC into Si$_3$N$_4$, 0·5 MPa pressure of nitrogen is insufficient to make either reaction (4) or (5) proceed forward. At lower temperatures (e.g. 1400

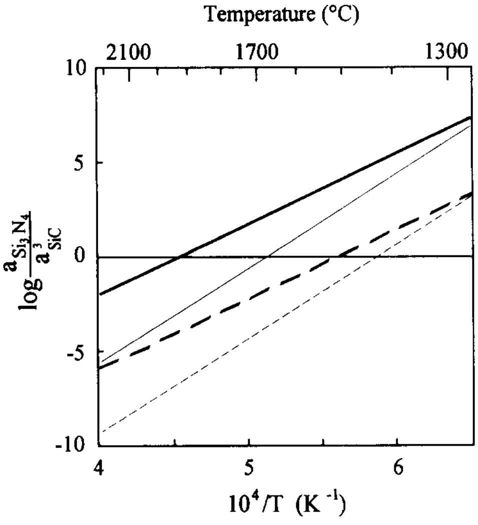

Fig. 8. Equilibrium between SiC and Si$_3$N$_4$, bold line representing α-Si$_3$N$_4$ and fine line β-Si$_3$N$_4$, at pressures of – – –, 0·5 MPa and ——, 50 MPa N$_2$ assuming $a_c = 1$, $P_{\text{O}_2} = 10^{-20}$ atm.

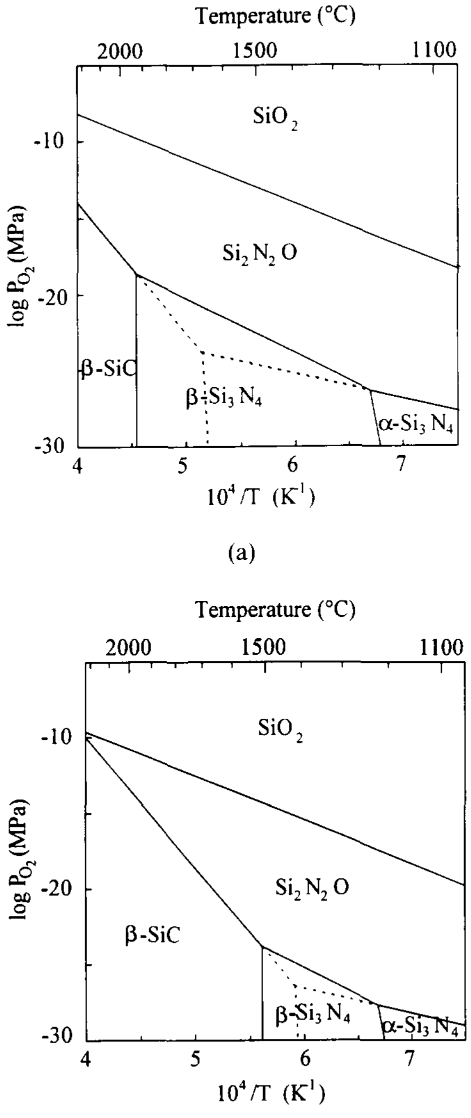

(a)

(b)

Fig. 9. Phase stability diagram of Si–C–N–O as a function of oxygen partial pressure and temperature at (a) 0·5 MPa N_2 and (b) 50 MPa N_2.

and 1450°C) Fig. 9 indicates that Si_3N_4 would be stable, if present. Nonetheless, since the specimens were constituted by 'pure' SiC no change was observed (see column for 0·5 MPa in Table 1), which therefore means that at these low temperatures the thermal activation for conversion is too small.

On the other hand, neglecting for the moment the type of Si_3N_4 present in the specimens, it may be seen that the data in Table 1 for the formation of Si_3N_4 at 50 MPa is well accounted for by considering the straight line for β-Si_3N_4 in Fig. 8, which indicates stability of β-Si_3N_4 up to ~1930°C. Again, at 1400 and 1450°C no change is observed, even at this high pressure, due to an insufficient thermal activation. The importance of temperature in the conversion process cannot be overemphasized since at 1800°C SiC is destabilized to be completely converted (see data for the interior of the specimen in Table 1) into Si_3N_4 and carbon. The amount of SiC observed on the surface is possibly due to a reaction between SiO and carbon encouraged during cooling by the proximity of the specimens to carbon sources like the crucible and the heating element.

In addition, the influence of pressure may be analyzed with the aid of numerical data for the amounts of Si_3N_4 observed in the core of the specimens at 1750°C. It may be seen that at 5 MPa the conversion process has already started, giving rise to a composite with a SiC/Si_3N_4 ratio of 85/15. At higher pressures, from 50 MPa upwards, the nitridation of SiC is very profuse and a composite with ratio of SiC/Si_3N_4 = 20/80 is then obtained. These results are also in accord with the theoretical calculations represented in Fig. 8.

It is noteworthy that all the specimens contain important amounts of α-Si_3N_4 after sintering. Besides, as illustrated in Table 3, the amounts of α-Si_3N_4 measured show an increasing tendency as either temperature or pressure are increased. This latter point was observed to be even more accentuated at the surface of the specimens where at a temperature of 1800°C and under a pressure of 50 MPa all Si_3N_4 formed is α-type.

This behaviour was somewhat unexpected, since, according to the data used for the construction of Fig. 8, and within the experimental range used in this work, β-Si_3N_4 is thermodynamically more stable than the corresponding α-type. This fact is also reflected by the phase stability diagrams, presented in Fig. 9, obtained through calculations using data available in the literature.[21]

According to the stability range for β- and α-Si_3N_4 indicated by these diagrams β-Si_3N_4 should have been observed under several conditions of pressure and temperature used in this work. Since this statement is contrary to the experimental observations, it has to be concluded that (at least in the absence of β-Si_3N_4 seeds) β-Si_3N_4

Table 3. Quantitative results in terms of α- and β-Si_3N_4, obtained from XRD traces after sintering of SiC powder compacts during 30 min under several combinations of temperature and pressure

Temperature (°C)	*Pressure (MPa)*				
	0·5	*5*	*50*	*75*	*200*
1400	NC	NC	NC		
1450	NC	NC	NC		
1500	NC		S-21-14 I-7-12		
1750	NC	S-48-25 I-7-8	S-60-23 I-61-26		I-59-30
1800			S-100-0 I-65-35		
1850		NC			

NC = no change observed, S = surface and I = interior. Numbers correspond to amounts measured for α-Si_3N_4 (first number) and β-Si_3N_4 (second number).

cannot be nucleated directly, the formation of the α-form, being necessary first, followed by the α → β transformation. Consequently, although β-Si_3N_4 is thermodynamically more stable, the α → β transformation is subjected to kinetic factors, it therefore being possible, as observed in this work, to obtain the α-type as a metastable phase after sintering.

According to these arguments the stability range for α-Si_3N_4, considered as a metastable phase, can be recalculated, neglecting the data corresponding to the β-form. The result of these calculations is represented in Fig. 9 by the broken lines in the diagrams which indicate an extended field of stability for α-Si_3N_4. Comparison of the experimental data with these metastable diagrams thus allows it to be seen, although not very accurately, that in quantitative terms, the tendencies shown by the experimental data can be reasonably well accounted for in terms of these theoretical calculations. In principle it can therefore be concluded that the reaction product after nitridation of SiC is α-Si_3N_4 and that β-Si_3N_4 is only observed after the α→β transformation has taken place.

Therefore the influence of alumina has to be understood as being a direct one upon lowering the activation energy required for the transformation. Since alumina is also observed to encourage densification, that is, facilitates material transport, it is likely that the α → β transformation requires a low viscosity liquid in which dissolution and reprecipitation can be eased.

On the other hand, microstructural analyses under the TEM did not show any evidence of an aluminium-rich secondary phase; however, this is not so surprising since both SiC and Si_3N_4 exhibit a certain solubility for aluminium, it therefore being possible that, after formation of a liquid, the aluminium ions migrate to the SiC and/or Si_3N_4 lattice.

Additionally, in contrast to some reports in the literature[22,23] from this study it can also be seen that in total absence of β-Si_3N_4 seeds, β-Si_3N_4 can still be formed, which therefore means that the α→β transformation does not necessarily proceed by the growth of existing β-Si_3N_4 nuclei, but, that it can be formed instead by nucleation from α-Si_3N_4.

5 Conclusions

From the results obtained in this work the following conclusions can be drawn:

(1) During high pressure nitridation of SiC-based green compacts a net weight gain is observed which consequently leads to an increase in density of the specimens accompanied by an extremely small shrinkage. This method shows therefore a great potential for producing SiC–Si_3N_4 composites by a non-shrinkage–densification route.

(2) The microstructure observed shows that the material mainly consists of SiC–Si_3N_4 grains in the nanosize range. The specimens were also observed to contain a small fraction of residual carbon which is constituted by graphite nanocrystals embedded in amorphous carbon areas.

(3) If residual carbon can be controlled this method could be used for the production of SiC–Si_3N_4 nanocomposites with selected SiC : Si_3N_4 ratios.

(4) Si_3N_4 formed from reaction between SiC and nitrogen at high temperature and pressure, nucleates directly as α-Si_3N_4, which remains as a metastable phase at room temperature; and β-Si_3N_4 only forms as a result of α→β transformation. Al_2O_3 additions encourage the α→β transformation and aid densification.

(5) The results obtained in terms of the phases observed in the specimens (SiC, α-Si_3N_4, β-Si_3N_4, etc.) after nitridation of SiC powder compacts at various combinations of temperature and nitrogen pressure may be interpreted to a reasonable degree of accuracy in terms of phase stability diagrams constructed through theoretical calculations using basic thermodynamic data previously reported in the literature.

Acknowledgements

The authors gratefully acknowledge the European Economic Community (BRITE Project Breu/0132-C (TT)) and the Ministerio de Educación y Ciencia of Spain for the economic support provided for the realization of this work.

References

1. Bowen, L. J., Weston, R. J., Carruthers, T. G. & Brook, R. J., Hot-pressing and α–β phase transformation in silicon nitride. *J. Mat. Sci.*, **13** (1978) 341.
2. Negita, K., Effective sintering aids for silicon carbide ceramics: reactivities of silicon carbide with various additives. *J. Am. Ceram. Soc.*, **69**(12) (1986) C-308.
3. Lange, F. F., Hot pressing behaviour of silicon carbide powders with additions of aluminium oxide. *J. Mat. Sci.*, **10** (1975) 314.
4. Shimada, M., Tanaka, A., Yamada, T. & Koizumi, M., Densification and phase transformation of Si_3N_4 by high pressure sintering. In *Ceramic Powders*, ed. P. Vincenzini, 1983, p. 871.
5. Iturriza, I., Castro, F. & Fuentes, M., Sinter and sinter-hip of silicon nitride ceramics with yttria and alumina additions. *J. Mat. Sci*, **24** (1989) 2047.

6. Lange, F. F., Effect of microstructure on strength of Si_3N_4–SiC composite systems. *J. Am. Ceram. Soc.*, **56** (1973) 445.
7. Greskovich, C., A gas pressure sintering process for producing dense Si_3N_4. In *Progress in Nitrogen Ceramics*, ed. F. L. Riley. Martinus Nijhoff Publishers, Boston/The Hague/Dordrecht/Lancaster, 1983.
8. Reddy, N. K., Silicon nitride–silicon carbide refractories produced by reaction bonding. *J. Am. Ceram. Soc.*, **74**(5) (1991) 1139.
9. Buljan, S. T., Baldoni, J. G. & Huckabee, M. L., Si_3N_4–SiC composites. *Am. Ceram. Soc. Bull.* **66**(2) (1987) 347.
10. Shalele, P. D., Petrovic, J. J., Murley, G. F. & Gac, F. D., Hot pressed SiC whisker/Si_3N_4 matrix composites. *Am. Ceram. Soc. Bull.*, **65** (1986) 351.
11. Greil, P., Tanaka, H. & Petzow, G., Sintering and hipping of silicon nitride–silicon carbide composite materials. *High Tech Ceramics*, ed. P. Vincenzini. Elsevier Science Publishers, B.V., Amsterdam, 1987, p. 1011.
12. Pick, A. N., Properties and applications of silicon carbide refractories. *Trans. Brit. Ceram. Soc.*, **78**(4) (1979) 13.
13. Herbert, D. B., Silicon carbide refractories—what is first quality. *Refract. J.* **40**(11) (1964) 456.
14. Washburn, M. E. & Loue, R. W., A silicon carbide refractory with a complex nitride bond containing silicon oxynitride. *Am. Ceram. Soc. Bull.*, **41**(7) (1962) 447.
15. Koch, C. C., The synthesis and structure of nanocrystalline materials produced by mechanical attrition: a review. *Nanostructured Materials*, **2** (1993) 109.
16. Niihara, K., Hiramo, T., Nakahira, A., Suganuma, K., Izaki, K. & Kawami, T., Nanostructure and thermomechanical properties of Si_3N_4/SiC composites fabricated from Si–C–N precursor powders. *J. Jap. Soc. Powder Metall.*, **36** (1989) 243.
17. Niihara, K., Suganuma, K., Nakahira, A. & Izaki, K., Interfaces in Si_3N_4–SiC nanocomposite. *J. Mater. Sci. Lett.* **9** (1990) 598.
18. Maeder, G., Ramon, Y., Thoral, G. & Barralis, J., Dosage par radiocristallographie X de l'austénite résiduelle dans des aciers 16 NCD 13 cémentés. Mémoires Scientifiques Revue Metallurgie, May, 1975, pp. 397.
19. Ekström, T. & Nygren, M., SiAlON ceramics. *J. Am. Ceram. Soc.* **75**(2) (1992) 259.
20. Wada, H., Wang, M. J. & Tien, T. Y., Stability of phases in the Si–C–N–O system. *J. Am. Ceram. Soc.*, **71**(10) (1988) 837.
21. Hendry, A., Structural ceramics: processing, microstructure and properties. In *11th Riso International Symposium on Metallurgy and Materials Science*, ed. J. J. Bentzen, J. B. Bilde-Sorensen, N. Christiansen, A. Horsewell & B. Ralph. (1990) p. 27.
22. Petzow, G. & Hoffmann, M. J., Grain growth studies in Si_3N_4 ceramics. In *Recrystallization 92 Materials Science Forum*, Vol. 113–15, ed. M. Fuentes & J. Gil Sevillano, 1992, p. 91.
23. Hermel, W., Herrmann, M. & Schubert, C., Have the limits of the development of β-Si_3N_4 materials already been reached? In *Third Euro-Ceramics*, Vol. 3, ed. P. Duran & J. F. Fernandez, 1993, p. 391.